



PERGAMON

Available online at www.sciencedirect.com

SCIENCE @ DIRECT®

International Journal of
**HEAT and MASS
TRANSFER**

International Journal of Heat and Mass Transfer 46 (2003) 4439–4451

www.elsevier.com/locate/ijhmt

Experimental study of nucleate boiling of halocarbon refrigerants on cylindrical surfaces

Gherhardt Ribatski, José M. Saiz Jabardo *

Departamento de Engenharia Mecânica-Escola de Engenharia de São Carlos, Universidade de São Paulo, Av. Trabalhador São-carlense, 400 Centro, 13566-590 Alameda Mariana, São Carlos, SP, Brazil

Received 5 August 2002; received in revised form 28 April 2003

Abstract

The present paper reports the results of an experimental investigation of saturated pool boiling of halocarbon refrigerants on cylindrical surfaces of different materials. Experiments covered a wide range of reduced pressures and heat fluxes, being carried out on copper, brass and stainless steel surfaces with different finishing conditions. The obtained results are discussed with regard to the controlled physical and operational parameters of the investigation. An empirical correlation is proposed in terms of reduced pressures. The performance of the correlation can be deemed adequate, considering that it compares well with experimental results of different authors.

© 2003 Elsevier Ltd. All rights reserved.

Keywords: Nucleate boiling; Heat transfer; Phase change; Halocarbon refrigerant

1. Introduction

Nucleate boiling has been under intense scrutiny since the early 1930s, when pioneering research studies came to light. This interest is justified in part by the heat transfer enhancement that this mechanism promotes on heated surfaces, and consequently by its potential in heat transfer applications. However, the associated heat transfer mechanism is a rather complex one what explains the significant amount of physical models proposed along the years and the attraction that it exerts to the scientific community. The difficulty stems in the fact that there is no generalized theory or model that adequately represents the phenomenon of nucleate boiling heat transfer. Generally speaking, nucleate boiling research has been traditionally approached by two different ways of analysis: (1) the investigation of the physical mechanism; (2) the development of correlations for the heat transfer coefficient based on either a physical in-

sight of the intervening phenomenon or a strictly empirical basis. Physical models tend to reproduce the particular mechanism that prevails under specific operational conditions of the boiling surface such as pressure, liquid subcooling, liquid/surface combination, geometry, and surface condition. As a result most of these correlations are strongly dependent on operational conditions not being amenable to generalizations, since they reproduce a particular view of the boiling phenomena. Thus, given the current state of the art, the investigation of the nucleate boiling phenomena is still needed to further deepen its understanding, specially with liquids characterized by low surface tension like the halocarbon refrigerants.

The material presented herein reports results from a comprehensive experimental investigation of boiling of halocarbon refrigerants on cylindrical surfaces. It covers a description of the experimental apparatus and procedures along with a parametric analysis of the obtained results. These include the effects of pressure, heat flux, and surface material and roughness for different refrigerants. In addition the paper also includes the development of a correlation based on the procedure proposed by Cooper [1]. Effects of parameters such as heat flux, fluid (refrigerant), pressure, and surface material and

* Corresponding author. Tel.: +55-16-273-9422; fax: +55-16-273-9402.

E-mail addresses: ribatskil@uol.com.br (G. Ribatski), mjabardo@sc.usp.br (J.M.S. Jabardo).

Nomenclature

| | |
|------------------|---|
| a | exponent of M |
| b_1, b_2 | exponents relative to Ra effects |
| c | specific heat, J/kg K |
| c_1, c_2 | exponents relative to pressure effects |
| D | diameter, mm |
| f_w | surface material parameter |
| g | gravitational acceleration, m/s ² |
| $(r_c)_{\min}$ | minimum cavity size for nucleation, μm |
| s | material surface parameter ($k_w \rho_w c_w$) |
| T | temperature, K |
| T_{sat} | saturation temperature, K |
| v | specific volume, m ³ /kg |
| Z_c | critical compressibility factor |
| h | heat transfer coefficient, W/m ² K |
| k | thermal conductivity, W/m K |
| M | molecular mass, kg/kmol |
| m | exponent of ϕ |
| m_1, m_2, m_3 | constants of the m correlation |

| | |
|-------|---|
| n/A | active nucleate site density, m ⁻² |
| p | pressure, kPa |
| Ra | arithmetical mean deviation of the profile, μm ; ISO 4287/1:1984 |
| R_p | maximum peak height of the profile, μm ; DIN 4762/1:1960 |

Greek symbols

| | |
|---------------|---|
| ΔT | surface superheat ($T_w - T_{\text{sat}}$), K |
| ε | relative deviation |
| ϕ | specific heat flux, W/m ² |
| ω | Pitzer acentric factor |
| θ | contact angle, ° |
| ρ | density, kg/m ³ |

Subscripts

| | |
|---|--------------------|
| r | reduced properties |
| w | wall |

roughness are considered and introduced into the correlation.

2. Experimental setup

The experimental setup comprises the refrigerant and cooling circuits. The refrigerant circuit is schematically shown in Fig. 1. The charge of refrigerant is basically contained in the boiler in which the liquid is kept at a reasonable level above the test surface (tube) so that the column head does not affect significantly the equilibrium saturation temperature. The cooling circuit is intended

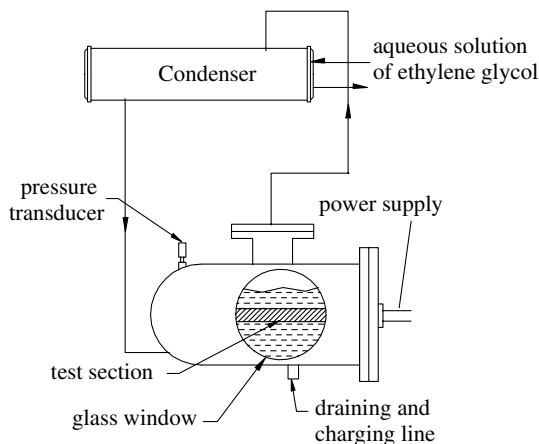


Fig. 1. Schematic diagram of the experimental apparatus.

to control the equilibrium pressure in the boiler by condensing the refrigerant boiled on the heating surface. The condensing effect is obtained by a 60% solution of ethylene glycol/water that operates as intermediate fluid between the condenser and the cooling system, not shown in Fig. 1. Depending on the operating pressure, the ethylene glycol/water solution is cooled by either a refrigeration circuit or water from a cooling tower.

The boiler is a 40 l carbon steel container with two lateral circular windows for visualization. It contains the boiling surface in addition to a 1500 W/220 V electrical heater, installed at the bottom, and two sheathed type T thermocouples. The boiler is also fitted with openings for connections to a pressure transducer, a safety valve (not shown in the figure), and vapor and liquid return copper lines, as shown in Fig. 1. The sheathed thermocouples are installed in such a way to measure and monitor the temperature of the liquid pool and the vapor in equilibrium with it. Under normal operating conditions, these thermocouples indicate temperatures very close to each other and to the saturation temperature at the boiler internal pressure measured by the pressure transducer.

The test (boiling) surface is placed in the middle of the boiler so that the boiling mechanism can easily be visualized through the glass windows. It is made up of a 19.0 mm diameter and 3.1 mm thick tube (copper, brass or stainless steel), a cut way view of it is shown in Fig 2. The test tube is supported by a brass piece which is thread attached to the flanged cover of the boiler. The electrical power to the boiling surface is controlled by a manually operated voltage converter and measured by a

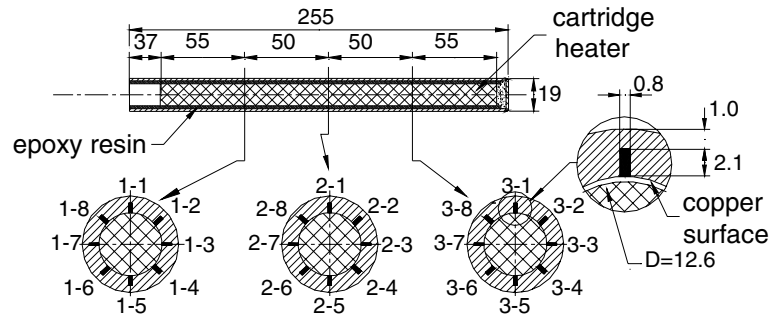


Fig. 2. Longitudinal and transversal cut views of the cylindrical heating surface. Measurements in mm.

power transducer. Surface temperature is measured through 30 AWG type T thermocouples installed in grooves carved by an electro-erosion process in locations indicated in Fig. 2 for the two copper surfaces used in the experiments. In the case of the brass and stainless steel surfaces, only four thermocouple junctions have been used, placed in the midway section and separated from each other by 90° along the circumference. Thermocouples are kept in place by a conductive epoxy resin. Electrical signals from the transducers are processed by a data acquisition system which includes two 12 bit A/D converter boards with 16 channels each, and three connection panels.

3. Experimental procedure

The boiling surface used to be treated prior to the beginning of the tests. Sandpaper scales with mesh size varying in the range from 220 to 1200 were used to obtain the final surface roughness and applied through a regular late machine run at 1200 rpm. Experiments were also conducted with a polished surface, which required a special treatment, and a sand blast surface. After such a treatment, the boiling surface used to be thoroughly cleaned with a solvent (normally refrigerant R-11) and the roughness measured at 10 randomly selected regions before attaching it to the boiler. After testing, other 10 randomly selected regions of the boiling surface were again taken for roughness measurement so that conditions of the surface before and after the tests could be compared. The roughness was measured in terms of the CLA arithmetic average, R_a . The treatment suggested above allowed experiments to be run in the range of surface roughness, R_a , between 0.02 ± 0.01 and $3.3 \pm 0.4 \mu\text{m}$.

The internal surface of the boiler used to be cleaned and kept under a vacuum of less than 2 kPa during a period of 12 h before attaching the boiling surface and introducing the refrigerant. Tests were conducted under saturated conditions of the refrigerant. The datum point

would only be logged if the readings of the sheathed thermocouples were close enough (within 0.2 K) to each other and to the saturation temperature corresponding to the boiler pressure. For analysis purposes, the saturation temperature of the pool was determined as the average of the readings of the sheathed thermocouples. Care was exercised in determining the surface temperature by taking into account the thermal resistance of the copper wall between thermocouple location and the actual boiling surface. In addition, axially located thermocouples helped in evaluating axial heat conduction. It has been determined that in the location corresponding to section 2 of the test tube, Fig. 2, the axial heat flux was negligibly small.

Gorenflo et al. [2] pointed out that the extreme temperatures occur at top and bottom of the heating surface a trend that has been confirmed by the experimental results. Thus the temperature indicated by the thermocouple located midway between those at top and bottom of the heating surface would correspond to the circumferential average temperature, as suggested by Kang [3]. As a result, only the intermediate thermocouple readings of the midway cross-section of the heating surface were considered for analysis purposes. A thorough discussion of the surface temperature evaluation can be found in Ribatski [4].

Tests were conducted by gradually increasing the heat flux up to its predicted maximum. Once the maximum was attained, the heat flux was gradually reduced down to zero. Only downward heat flux data were considered for analysis purposes. Several procedures were tried to check for possible side effects on the results. One of them consisted in keeping the boiling surface active for some time before logging data whereas in the other the heating of the surface started directly from the maximum heat flux. Results from these heating procedures were very close to call.

Instruments were calibrated and the uncertainty of measured parameters evaluated according to the procedure suggested by Abernethy and Thompson [5] with results summarized in Table 1.

Table 1
Uncertainty of measured and calculated parameters

| Parameter | Uncertainty |
|---|---------------------|
| Minimum heat flux, $\phi = 0.60 \text{ kW/m}^2$ | $\pm 1.8\%$ |
| Maximum heat flux, $\phi = 120 \text{ kW/m}^2$ | $\pm 0.3\%$ |
| Heat transfer area | $\pm 0.3\%$ |
| Wall temperature | $\pm 0.2 \text{ K}$ |
| Saturation temperature | $\pm 0.2 \text{ K}$ |
| Superheating | $\pm 0.3 \text{ K}$ |
| Heat transfer coefficient, $h = 2.3 \text{ kW/m}^2 \text{ K}$, R-123, $p_r = 0.011$, $Ra = 0.16 \text{ }\mu\text{m}$, copper, $\phi = 114 \text{ kW/m}^2$ | $\pm 1.3\%$ |
| Heat transfer coefficient, $h = 4.2 \text{ kW/m}^2 \text{ K}$, R-134a, $p_r = 0.260$, $Ra = 2.5 \text{ }\mu\text{m}$, copper, $\phi = 2.27 \text{ kW/m}^2$ | $\pm 20\%$ |

4. Parametric analysis of results

A fairly good amount of data points have been gathered under the investigation reported herein. A total of 2600 valid data points have been raised, involving the following conditions for cylindrical surfaces of 19 mm diameter:

- *Refrigerants:* R-11, R-123, R-12, R-134a, and R-22,
- *Reduced pressures:* varying in the range between 0.008 and 0.260,
- *Surface average roughness:* varying in the range between 0.02 and $3.3 \text{ }\mu\text{m}$,
- *Surface material:* copper, brass, and stainless steel.

The above physical parameters constitute the set of conditions whose effect over nucleate boiling has been the main thrust of the investigation reported in this paper. A summary of the obtained results is presented in connection with these effects in the following sections.

4.1. Refrigerant

The relative performance of refrigerants under nucleate boiling conditions depends upon complex interactions between their thermodynamic and transport properties with surface material and condition. These interactions will be further discussed in the subsequent sections. As a first approximation, results indicate that volatile refrigerants, such as R-12, R-134a, and R-22, present higher heat transfer coefficient than their less volatile counterparts, such as R-11 and R-123, at the same reduced pressure.

4.2. Pressure

In the past there has been a number of publications dealing with pressure effects in nucleate boiling. Pressure affects directly two bubbles related parameters: frequency and active nucleate site density. It seems that heat transfer enhancement with pressure is closely related to the increment of these parameters. The combined effect of pressure and surface roughness over the

boiling curves of lower pressure refrigerants R-11 and R-123 is displayed in Fig. 3(a) and (b). The degree at which pressure affects the boiling curve depends upon, among other things, the pressure level itself, the refrigerant, and surface material and condition. In Fig. 3(a), the boiling curves of refrigerants R-11 and R-123, for a surface average roughness of $0.16 \text{ }\mu\text{m}$, are very close to each other at the reduced pressures indicated in the figure, confirming a trend previously observed by Webb

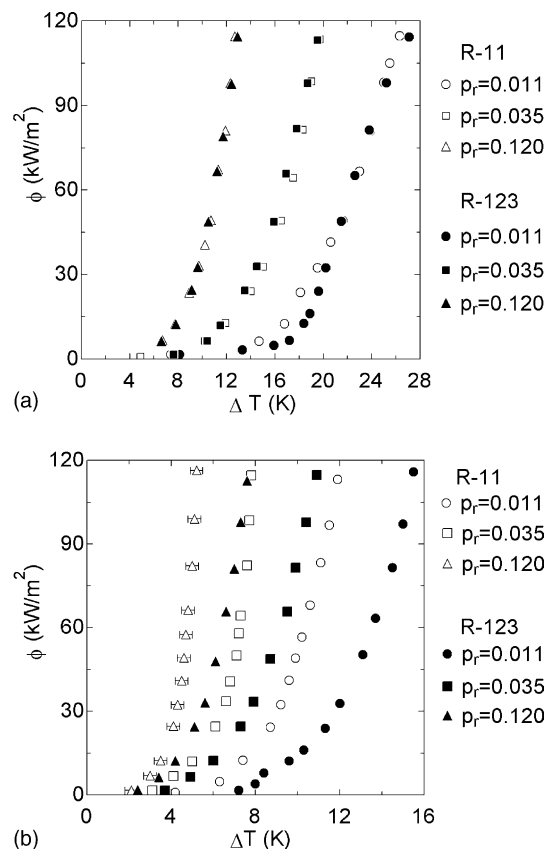


Fig. 3. Boiling curves for low pressure refrigerants R-11 and R-123 boiling on a copper surface: (a) $Ra = 0.16 \text{ }\mu\text{m}$; (b) $Ra = 2.3 \text{ }\mu\text{m}$, for R-11, and $Ra = 3.3 \text{ }\mu\text{m}$, for R-123.

and Pais [6]. Two interesting trends must be considered regarding the boiling curves of Fig. 3(b):

- (1) Despite a smoother boiling surface ($Ra = 2.3 \mu\text{m}$ against $Ra = 3.3 \mu\text{m}$), refrigerant R-11 curves are steeper than the ones corresponding to R-123 for the same reduced pressure. Thus considering the combined results of Fig. 3(a) and (b), it can be concluded that surface roughness affects more nucleate boiling heat transfer of R-11 than that of R-123.
- (2) On the other hand, it can be noted that the R-123 boiling curves, though less steeper, tend to come closer to the R-11 ones for higher reduced pressures, implying that nucleate boiling of the former refrigerant is affected more by pressure when boiling on rough surfaces.

4.3. Surface roughness

The effect of the heating surface roughness over the boiling curve, previously demonstrated in Fig. 3(a) and (b), is clearly shown in Fig. 4 for refrigerants R-22 and R-134a. It can be noted that the boiling curves of refrigerant R-134a are affected more by the surface average roughness than the ones for R-22. Similarly to Fig. 4, when passing from Fig. 3(a), for a smooth surface, to Fig. 3(b), obtained for fairly roughened heating surfaces, the boiling curves become steeper, indicating a significant heat transfer enhancement, with stronger effects in the case of refrigerant R-11. In general, nucleate boiling heat transfer increases with the surface roughness. It is a well-known fact that this enhancement is related to the active site density increment, since on roughened surfaces the range of cavity sizes available for nucleation is wider. It has been suggested elsewhere that the increment in the active site density diminish with the average

roughness, as the surface becomes rougher [7]. In addition, Kurihara [7] suggested the occurrence of a surface roughness limit above which there is no further heat transfer enhancement. This limit has been confirmed by results obtained under the present investigation with sand blasted surfaces.

Surface roughness effects seem to be related to the minimum cavity size for nucleation, $(r_c)_{\min}$, associated to the boiling fluid, according to nucleation models such as the ones by Hsu [8] or Han and Griffith [9]. Table 2 has been prepared in order to check for this trend. Values of the $(r_c)_{\min}$ from the Han and Griffith model for each refrigerant can be found in the second row of the table for a heat flux of 50 kW/m^2 and a reduced pressure of 0.064. The third row includes the relative variation of the experimental heat transfer coefficient, for the same heat flux and reduced pressure as above, defined as

$$\Delta h_{\text{relative}} = \frac{[h(Ra_2) - h(Ra_1)]/h(Ra_1)}{(Ra_2 - Ra_1)/Ra_1} \quad (1)$$

where Ra_1 is the minimum value of the average roughness in the experiments and Ra_2 is an arbitrary one which, in this case, was assumed as being equal to $0.5 \mu\text{m}$. The experimental minimum average roughness is equal to $0.16 \mu\text{m}$, for the lower pressure refrigerants (R-11 and R-123), and $0.08 \mu\text{m}$, for the higher pressure ones (R-134a, R-12, and R-22). The values of $\Delta h_{\text{relative}}$ of Table 2 indicate that surface roughness affects more nucleate boiling heat transfer of refrigerant R-11 than that of R-123. Among the high-pressure refrigerants, R-12 presents the highest and R-22 the least relative variation of the heat transfer coefficient. The observed trends regarding the effects of the average roughness over the heat transfer coefficient are similar to those of $(r_c)_{\min}$ in Table 2. Thus, as a first approximation, there seems to be a relationship between the effect of the surface roughness over the heat transfer coefficient and the associated $(r_c)_{\min}$ for each refrigerant. This result seems to be in agreement with Kurihara's model [7], according to which, the variation of the active nucleate site density is proportional to $\exp[-1/(r_c)_{\min}]$.

4.4. Heating surface material

The effect of the heating surface material depends on the boiling fluid. The boiling curves of Fig. 5(a) show the effect of the surface material for refrigerant R-11. Brass surfaces are thermally more efficient for this refrigerant than the copper and stainless steel ones, since the boiling curves for this material are steeper. This is not the case for refrigerant R-12 whose boiling curves for different reduced pressures on brass and copper surfaces are shown in Fig. 5(b). Clearly the boiling curves for brass and copper are closer than in the previous case. Similar behavior has been found for the other refrigerants

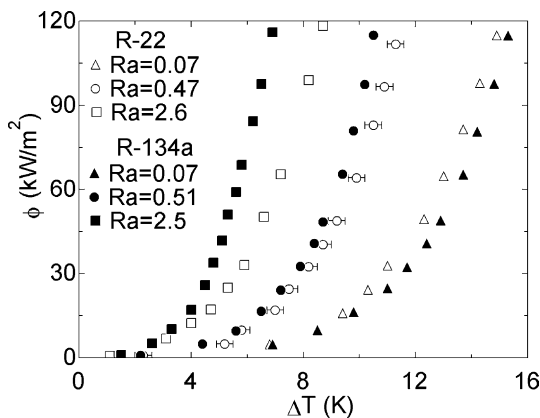


Fig. 4. Boiling curves of high-pressure refrigerants R-22 and R-134a for different surface conditions and at a reduced pressure of 0.064 (Ra in μm).

Table 2

Values of $(r_c)_{\min}$ for different refrigerants at $\phi = 50 \text{ kW/m}^2$ and $p_r = 0.064$ according to the Han and Griffith model along with values of the relative variation of the heat transfer coefficient, $\Delta h_{\text{relative}}$

| | R-11 | R-123 | R-12 | R-22 | R-134a |
|--|------|-------|------|------|--------|
| $(r_c)_{\min}$ (μm) | 0.37 | 0.34 | 0.29 | 0.25 | 0.26 |
| $\Delta h_{\text{relative}}$, Eq. (1) | 0.18 | 0.15 | 0.09 | 0.06 | 0.08 |

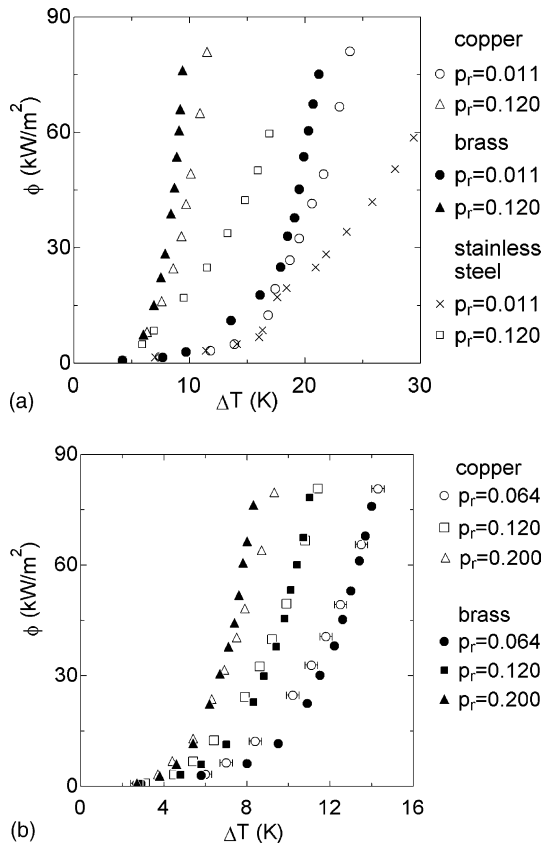


Fig. 5. Boiling curves of (a) R-11, $Ra = 0.16 \mu\text{m}$; (b) R-12, $Ra = 0.07 \mu\text{m}$.

considered in the present investigation. As a general rule (R-12 is an exception), the nucleate boiling heat transfer coefficient is higher for brass surfaces diminishing

Table 3

Comparison of the variation of the experimental heat transfer coefficient ($\phi = 50 \text{ kW/m}^2$, $Ra \approx 0.50 \mu\text{m}$) with the change of surface material

| | | R-11 | R-123 | R-12 | R-22 | R-134a |
|-----------------------------------|----------------------------------|------|-------|------|------|--------|
| Experimental ($p_r = 0.064$) | $h_{\text{brass}}/h_{\text{Cu}}$ | 1.24 | 1.12 | 0.80 | 1.17 | 1.31 |
| | $h_{\text{SS}}/h_{\text{Cu}}$ | 0.71 | 0.69 | – | – | 0.81 |
| Eq. (2), [12] ^a | $h_{\text{brass}}/h_{\text{Cu}}$ | | | 0.71 | | |
| | $h_{\text{SS}}/h_{\text{Cu}}$ | | | 0.45 | | |

^a Effects of surface material variation according to the correlation proposed by Gorenflo et al. [12].

slightly for copper and still further for stainless steel, other physical parameters kept equal. In addition, the degree of surface material effects depends on the particular boiling fluid as shown in Fig. 5(a) and (b). Actually, this behavior seems to be related to the so-called surface/fluid effect suggested by Rohsenow [10].

Two physical mechanisms could be related to effect of the surface material:

- (1) *Thermal inertia*, related to transient effects. It affects the weighting and growing times of the bubbles, and possibly the active site density, as suggested by Man et al. [11], as a result of interaction effects between neighboring sites.
- (2) *Boiling liquid wettability*, with effects over the weighting and growing times of the bubbles and the active site density as well.

The independent effect of the first mechanism, as some of the current published nucleate boiling correlations seem to imply, does not conform with trends displayed by the experimental results, as shown in Table 3. It can be noted in the second and third rows that the experimental heat transfer enhancement of brass and stainless steel with respect to copper surfaces ($h_{\text{surface}}/h_{\text{Cu}}$) depends on the particular boiling fluid, as previously shown in Fig. 5(a) and (b). The last two rows include surface material effects according to the correlation proposed by Gorenflo et al. [12], which can be reduced to the following equation:

$$\frac{h_{\text{surface}}}{h_{\text{Cu}}} = \left(\frac{s_{\text{surface}}}{s_{\text{Cu}}} \right)^n \tag{2}$$

where n is equal to 0.25 and the parameter s is defined as the product $k_w \rho_w c_w$. It can be noted that, according to

Eq. (2), surface material effects do not depend on the particular boiling fluid.

In conclusion, thermal inertia parameters of the heating surface material do not seem to adequately reproduce observed trends of the experimental results. In addition, given that the values of density and specific heat of the materials considered in this paper are relatively close, the significant surface material parameter would be the thermal conductivity, k_w , whose effect over nucleate boiling heat transfer is marginal according to Cooper [13]. Thus, as suggested previously, the effect of the surface material over nucleate boiling heat transfer depends strongly on the boiling fluid, with the material transport properties, specially the conductivity, playing a marginal role, at least for the materials and wall thickness considered in this paper.

4.5. Other effects

A peculiar behavior has been noted when low pressure refrigerants (R-11 and R-123) boiling on the stainless steel surface at a relatively low heat fluxes and reduced pressures. The plot of Fig. 6 shows a detail of the boiling curve of refrigerant R-123 in the low heat flux range at the reduced pressure of 0.011. The plots shown in this figure correspond to data obtained in different days, at the same reduced pressure and surface material and condition, by reducing the heat flux from a given maximum down to zero. A significant deviation can be noted between the curves in the heat flux range between 10 and 20 kW/m². The curve corresponding to experiment 1 presents a clear discontinuity at about 13 kW/m². It is interesting to note that beyond the anomalous region both curves coincide, as expected.

In order to investigate in detail this behavior, close examination of images from tapes taken with a regular

video camera were carried out along with visual observations through the windows of the boiling vessel. It has been found out that in the anomalous region, nucleate boiling occurs in an intermittent fashion, with clusters of bubbles appearing and disappearing in different regions of the heating surface. It has been observed that the active site density is higher and the bubbles size smaller in the uppermost region with respect to those at the bottom of the boiling surface. A possible explanation for this behavior could be related to natural convection effects, which would cause the surface temperature to increase from bottom to top. Higher temperatures at the top of the surface would prompt higher bubble frequency and active nucleate site density along with smaller bubbles. The low temperature at the bottom would inhibit nucleation and increase the weighting time of the bubble cycle, reducing the frequency and possibly allowing for the increment of the bubble size. Difficulty in slipping away along the surface and increased surface tension could contribute further to enhance the bubble size. Bubble cycles on the wall of the order of 60 s have been observed when refrigerant R-123 boils on the stainless steel surface for a heat flux of 10 kW/m² and reduced pressure of 0.011. Under these conditions, the bottom surface thermocouple experienced temperature variations of the order of 2 °C.

This anomaly has also been observed on the brass surface, though not as apparent as in stainless steel. In the case of copper surfaces this behavior seems to be almost insignificant. It seems that the lower thermal conductivity of stainless steel and brass inhibits heat conduction along the perimeter of the heating wall, allowing for higher temperature differences between the top and bottom, what would enhance the aforementioned phenomenon.

5. Comparison with correlations

The results discussed in the previous sections, based on data from the present investigation, generally tend to confirm fairly well established nucleate boiling heat transfer concepts and trends. In order to quantitatively evaluate these results, the following correlations have been considered for comparison purposes: Cooper [13], Stephan and Abdelsalam [14], and VDI-Heat Atlas [15], corrected by Gorenflo et al. [12]. The comparison has been made in terms of the average deviation, defined as

Average deviation

$$= \frac{1}{n} \sum_{i=1}^n \frac{|(\text{Correlation value}) - (\text{Experimental value})|}{(\text{Experimental value})} \quad (3)$$

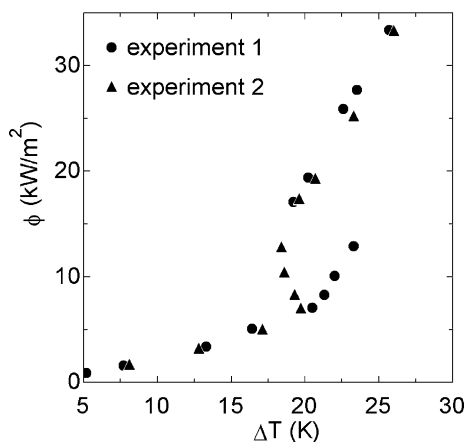


Fig. 6. Detail of the partial nucleate boiling region for R-123, $Ra = 0.16 \mu\text{m}$, $p_r = 0.011$ on the stainless steel surface.

Average deviations of the calculated with respect to the experimental heat transfer coefficient for the three correlations, extensive to the complete data set, is of the order of 25%, 22%, and 23%, respectively. These figures could be deemed as reasonable, though slightly high, given the relatively wide range of operational conditions and the different refrigerants involved in the present data. It would be interesting to show at this point how individual data points behave with respect to the correlation of Stephan and Abdelsalam, the one with the least average deviation. Calculated versus experimental heat transfer coefficient is shown in Fig. 7. It can be noted that the experimental heat transfer coefficient is generally higher than the one from Stephan and Abdelsalam correlation. The same trend has been found for the heat transfer coefficient from the Cooper's and VDI Heat-Atlas correlations, though their average deviations are slightly higher (25% and 23% against 22%).

Contrary to the other two, the modified VDI-Heat Atlas [15] correlation includes the effect of the heating surface material as suggested by Gorenflo et al. [12]. In order to evaluate the performance of this correlation with respect to surface material, the relative deviation, defined as $100 [h(\text{Correlation}) - h(\text{Experimental})] / h(\text{Experimental})$, of the calculated with respect to the experimental heat transfer coefficient has been plotted against the reduced pressure for data points corresponding to refrigerant R-134a, as shown in Fig. 8. Data points have been represented by different symbols to discriminate surface roughness and material. The following remarks could be drawn from a detailed analysis of this figure:

- (1) The modified VDI-Heat Atlas correlation tends to under predict the heat transfer coefficient on the

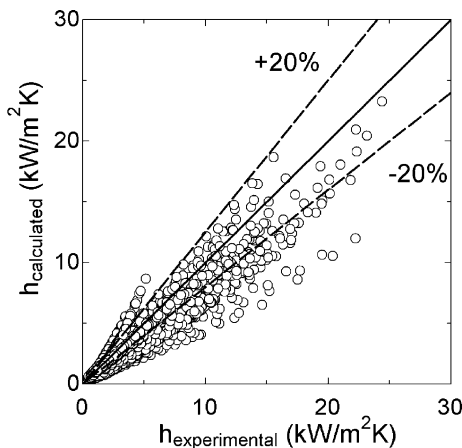


Fig. 7. Comparison of the calculated heat transfer coefficient through the Stephan and Abdelsalam [14] correlation with present experimental results for the complete set of data points.

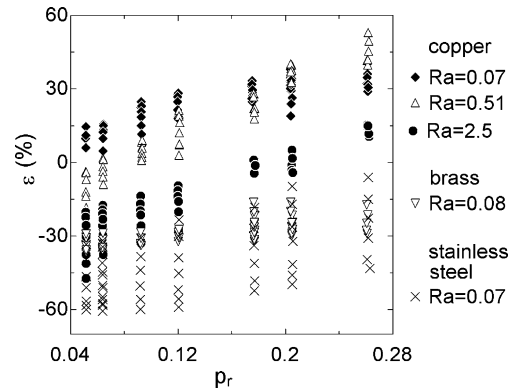


Fig. 8. Variation with p_r of the relative deviation, ε , of the VDI-Heat Atlas [15] calculated with respect to the experimental heat transfer coefficient, for refrigerant R-134a (Ra in μm).

stainless steel and brass surfaces. It can be noted that, for stainless steel and brass surfaces, the correlation compares poorly with the experimental results at lower reduced pressures, the performance improving with pressure. Opposite trend can be noted for the copper surfaces.

- (2) For copper surfaces, the correlation under predicts the heat transfer coefficient of surfaces with higher average roughness and over predicts it for lower average roughness. The previously suggested combined effect of the reduced pressure and surface roughness over heat transfer is not contemplated in the correlation, what explains the distinct variation of ε with the surface roughness for copper surfaces.
- (3) As a general rule, the relative deviation, ε , increases with the reduced pressure for each surface material and average roughness.

6. An empirical correlation

6.1. Fundamentals

Cooper [1] and Ribatski and Saiz Jabardo [16] have shown that, after some manipulation, current nucleate boiling heat transfer correlations can be reduced to the following general form:

$$\frac{h}{(\phi)^m} = Cgf(\theta) \left[\prod_{i=1}^n (\text{Fluid parameters})^{a_i} \right] \times \left[\prod_{i=1}^n (\text{Surface parameters})^{b_i} \right] \times \left[\prod_{i=1}^n (\text{Transport properties})^{c_i} \right] \quad (4)$$

It is interesting to note that the exponent, m , of the heat flux in the left hand side term assumes values close to 0.7 for most of the known correlations [10,14,15,17–21]. The function $f(\theta)$ is related to the surface tension of the liquid and to the characteristics of the surface material/liquid interaction whereas the *fluid parameters* can either involve a molecular parameter or an empirical constant. The surface parameters are related to the actual material and finishing of the heating surface. Finally, using arguments from the Law of Corresponding States, the last term of the right hand side can be reduced to an expression involving just reduced pressures and temperatures, as suggested by Cooper [1]. Ribatski and Saiz Jabardo [16] obtained simple yet accurate correlations for the saturated liquid and vapor transport properties of refrigerants in terms of reduced pressures and temperatures. Actually these correlations fit adequately the effect of either pressure or temperature over the saturated transport properties when given in terms of either $p_r(1 - T_r)$ or $p_r[-\log_{10}(p_r)]$. It is interesting to note that properties such as the surface tension and the latent heat of vaporization tend to zero at the critical state, and as a result must be written in terms of powers of $(1 - T_r)$. In addition, it must be noted that for most of the halo-carbon refrigerants the surface tension varies linearly with T_r .

Eq. (4) can further be reduced substituting the term involving the transport properties by a function of reduced pressures and/or temperatures. Since, in the present case, saturated conditions prevail, pressure and temperature are dependent properties for a pure substance, and, as a result, transport properties and their products could be reduced to a function of either reduced pressure or temperature. Thus, Eq. (4) could be reduced to the following general expression:

$$\frac{h}{(\phi)^m} = Cg f(\theta) \left[\prod_{i=1}^n (\text{Fluid parameters})^{a_i} \right] \times \left[\prod_{i=1}^n (\text{Surface parameters})^{b_i} \right] f(p_r; T_r) \quad (5)$$

In the next sections, the terms of Eq. (5) will be thoroughly discussed in order to obtain a simple form that fits the experimental results with reasonable accuracy.

6.2. Correlation parameters

6.2.1. Heat flux

The exponent m of the heat flux in the left hand side of Eq. (5) is closely related to the slope of the boiling curve. Thus it depends on the particular boiling fluid, the pressure, and the surface material and finishing. Cooper [13] initially suggested a linear relationship between this exponent and the reduced pressure. However, given the insignificant improvement in the fitted results

obtained by this approach, he opted for a constant value. Gorenflo et al. [12] tried to correlate the exponent m in terms of Ra and $p_r^{0.3}$, concluding that the effect of Ra over the accuracy of the proposed heat transfer correlation was insignificant. Present experimental results for the copper surfaces have shown that m varies approximately in the range between 0.7 and 0.87 for the refrigerants and the range of pressures considered in this paper, decreasing with the latter. Similar trend has been obtained for the stainless steel and brass surfaces.

6.2.2. Fluid parameter

Fitting generalized nucleate boiling heat transfer correlations to experimental results has been a difficult task when the identity of the particular boiling fluid is not taken into consideration. It has been shown that the introduction of a molecular parameter characteristic of the fluid improves the accuracy of the correlation [13,22]. Cooper [13] suggested the molecular mass, M , whereas others like Leiner [22] opted for equations involving the critical compressibility factor, Z_c , which is directly related to the Pitzer acentric factor, ω [23]. In order to check for the degree of correlation between the heat transfer coefficient and the molecular parameter associated to the particular refrigerant, the heat transfer coefficient has been evaluated for different refrigerants and conditions using different correlations from the literature. Though not shown in the present paper, the resulting heat transfer coefficients have been plotted in terms of both molecular parameters, M and ω , associated to each refrigerant, with the following conclusions having been drawn:

- (1) The heat transfer coefficient diminishes with M for most of the correlations [10,17–21], except for the Stephan and Abdelsalam [14] correlation.
- (2) A significant correlation can be noted between h and M .
- (3) Contrary to the molecular mass effect, ω does not seem to correlate the heat transfer coefficient in a discernible way.

Based on these arguments, the molecular mass has been chosen as the molecular parameter associated to the refrigerant, though both molecular parameters have been independently checked in the development of the correlation.

6.2.3. Average roughness of the heating surface

It has been previously noted that the effect of surface roughness depends on the particular reduced pressure range. In other words, the surface roughness, characterized here by Ra , interacts with pressure in such a way that its effect over the boiling curve is stronger at lower than at higher reduced pressures. Similarly, roughness can affect differently nucleate boiling heat transfer,

depending on the material of the heating surface. As a general rule, heat transfer correlations are based on the separation of effects grouping them in a general form similar to Eq. (5). In the present analysis only the effect of roughness and reduced pressure will be combined in a single parameter, following previous considerations made specially by Cooper [13] and Gorenflo et al. [12]. In order to do so, several equations involving Ra to p_r could be devised in such a way to make the roughness effect more significant in the lower range of reduced pressures. Some of these equations have been considered and checked for their effectiveness in the development of the proposed correlation.

6.2.4. Heating surface material

Some of the proposed correlations include the effect of the heating surface material through the group $(k_w \cdot \rho_w \cdot c_w)$, related to transient heat conduction effects in the material. Due to the lack of enough experimental information regarding these effects, an in depth analysis of this group has not been done in the present investigation. However, as previously mentioned, present results clearly suggest a combined surface/liquid interaction. Thus, for simplification purposes, a material dependent coefficient will take on heating surface material effects.

6.3. Procedure

The procedure starts with the selection of the set of experimental data to be used in the development of the correlation. Only data on the downward direction of heat fluxes down to the minimum boiling heat flux have been considered for analysis. The minimum heat flux has been arbitrarily chosen equal to 4 kW/m².

Table 4 includes all the forms of the parameters of Eq. (5) that have been considered in the present investigation. All possible combinations have been correlated, totaling 45 different forms. The chosen correlation is the one that allowed for the best fitting of the experimental data. Criteria used in the decision are as follows: (1) individual absolute average deviation for each re-

frigerant, reduced pressure and surface material lower than 15%; (2) behavior of each parameter compatible with the expected physical phenomenon; (3) simplicity; (4) lower overall absolute deviation of correlation with respect to experimental results. It must be noted that these criteria are mostly objective though the third one involves some sort of subjectivity.

The following steps have been followed in the fitting procedure of each of the forms of Table 4:

(1) *Heat flux exponent*: Each boiling curve was fitted with equations of the type: $h = (\text{Constant})\phi^m$. The resulting sets of m values were fitted to obtain m_1 , m_2 , and m_3 according to the forms of Table 4. For the first two cases of Table 4, corresponding to linear and exponential forms, the m_1 has been assumed equal to 0.9, a value previously suggested by Gorenflo et al. [12] and close to the highest experimental one, 0.87.

(2) *Reduced properties*: The reduced properties involve different combinations of p_r and T_r as shown in line two of Table 4 (reduced properties). By writing the forms of the group h/ϕ^m in terms of each of the forms, the values of exponents c_1 and c_2 can be determined.

(3) *Surface roughness*: The values of b_1 and b_2 can be determined in a similarly manner as in item (2), but, in this case, correlating the group $h/[(\text{Heat flux effects}) (\text{Reduced properties})]$ in terms of one of the forms of the surface roughness effects of Table 4.

(4) *Molecular parameter*: Different values of a can be determined, corresponding to different combinations of the previous groups, by following a procedure similar to the preceding steps. The Pitzer acentric factor, ω , has also been considered as previously suggested. However, a correlation between $h/[(\text{Heat flux effects}) (\text{Reduced properties}) (\text{Surface roughness effects})]$ and ω has not been found. On the other hand, the molecular mass displays a clear trend for the three surface materials considered in this investigation, what prompted its choice as molecular parameter associated to the boiling refrigerant.

(5) *Surface material*: The coefficient corresponding to each material was obtained by averaging the resulting values of the group: $h/[(\text{Heat flux effects}) (\text{Reduced properties})(\text{Surface roughness effects})(\text{Molecular mass})]$.

Table 4
Different forms of Eq. (5) parameters

| Parameter | Forms of to correlate the distinct parameters | | |
|---------------------|--|-----------------------------------|--|
| Heat flux | $\phi^{m_1 - m_2 p_r^{m_3}}$ | $\phi^{m_1 - m_2 p_r}$ | ϕ^{m_1} |
| Reduced properties | $p_r^{c_1} T_r^{c_2}$ | $p_r^{c_1} (1 - T_r)^{c_2}$ | $p_r^{c_1} (-\log p_r)^{c_2}$ |
| Surface roughness | $(Ra/5)^{b_1[-\log(p_r)]}$ | $Ra^{b_1} (Ra/5)^{b_1 - b_2 p_r}$ | $(Ra/5)^{b_1(1 - p_r)} p_r^{b_1 + b_2[-\log(Ra)]}$ |
| Molecular parameter | M^a | | |
| Surface material | Characteristic coefficient of the surface material | | |

The following expression has been found to meet the proposed conditions for the optimum correlation:

$$\frac{h}{\phi^m} = f_w p_r^{0.45} [-\log(p_r)]^{-0.8} Ra^{0.2} M^{-0.5} \quad (6)$$

where

$$m = 0.9 - 0.3p_r^{0.2} \quad (7)$$

The heat surface material parameter, f_w , assumes the following values for the materials considered in this paper:

- copper: 100
- brass: 110
- stainless steel: 85

7. Evaluation of the proposed correlation

The absolute (relative) average deviation of correlation with respect to experimental results, defined as Eq. (3), is considered as the reference parameter in the evaluation of the proposed correlation. Table 5 presents average deviations for different sets of experimental data, corresponding to individual surface materials, refrigerants and Ra ranges in addition to the overall. Deviations in Table 5 might be biased by the number of data points of each data set, and, as a result, Eq. (6) might correlate better data sets with higher number of data points. In any case, the proposed equation correlates experimental data with a reasonable accuracy considering the number of refrigerants, surface conditions and materials, and the range of operating conditions implicit in the results shown in Table 5. The correlation also captures odd behaviors such as the one experienced by refrigerant R-12. In fact, the heat transfer coefficient associated to refrigerant R-12 diminishes when a boiling copper surface is substituted by a brass one, a trend opposite to that of the other refrigerants. This behavior along with the reduced number of data points associated to R-12 might be responsible

for the higher average deviations related to this refrigerant in Table 5.

Table 5 shows the effect of the boiling surface roughness over the associated average deviation. As a general rule, the average deviation tends to increase with Ra . This trend might be related to the strong pressure/roughness interaction at higher values of Ra and lower reduced pressures. Thus, as a first glance, the use of one of the groups of the third line of Table 4, involving both Ra and p_r , should result in a more accurate correlation. However, a comparable accuracy was obtained with a correlation with a constant exponent (0.2 for the proposed correlation). It can also be noted that refrigerants R-11 and R-12 present higher deviations, probably as a result of the stronger effect of roughness, especially in the range of lower reduced pressures. Finally, it has been determined that, in general, lower reduced pressures tend to cause higher deviations, a trend which is probably related to the higher effect of the reduced pressure over the boiling curve in this range.

An overview of the correlation performance with respect to the experimental data can be seen in the plot of the calculated versus the experimental heat transfer coefficient of Fig. 9, with all the data points involved. It can be noted that most of the points fall well within the $\pm 20\%$ range.

The performance of the correlation has been evaluated through comparisons with experimental results obtained elsewhere. For that purpose, data from Silva [24], for refrigerants R-11, R-113, and R-114 boiling on a brass tube of 14.2 mm of external diameter, and Jensen [25], for refrigerant R-113 on a stainless steel tube of 12.7 mm of external diameter, have been considered. Since the surface roughness was not provided, Ra was estimated as the average roughness obtained by fitting the experimental data from these sources by the proposed correlation. An average surface roughness of 0.7 μm was obtained for the brass tube from Silva [24], and 1.3 μm for that from Jensen [25]. Fig. 10 displays the plot of calculated versus the experimental heat transfer coefficient for the combined data sets from Silva [24] and

Table 5
Average absolute deviations of Eq. (6) with respect to experimental results

| | Average deviation (%) | | | | | |
|-------------------------------|-----------------------|-------|--------|------|------|------------|
| | R-11 | R-123 | R-134a | R-22 | R-12 | Overall |
| Copper | 11.5 | 6.0 | 8.6 | 8.9 | 14.4 | 9.8 |
| Brass | 6.4 | 9.5 | 9.3 | 5.6 | 7.4 | 7.6 |
| Stainless steel | 10.4 | 12.4 | 12.2 | – | – | 12.5 |
| Overall | 10.1 | 8.2 | 10.0 | 8.1 | 12.2 | 9.6 |
| $Ra < 0.20 \mu\text{m}$ | 9.2 | 6.0 | 3.5 | 2.8 | 11.5 | 6.7 |
| $Ra \approx 0.50 \mu\text{m}$ | 4.9 | 6.1 | 10.2 | 12.6 | 15.1 | 11.1 |
| $Ra < 2.0 \mu\text{m}$ | 14.8 | 6.0 | 13.1 | 14.9 | – | 11.4 |
| Overall | 11.3 | 6.0 | 6.6 | 7.4 | 13.5 | – |

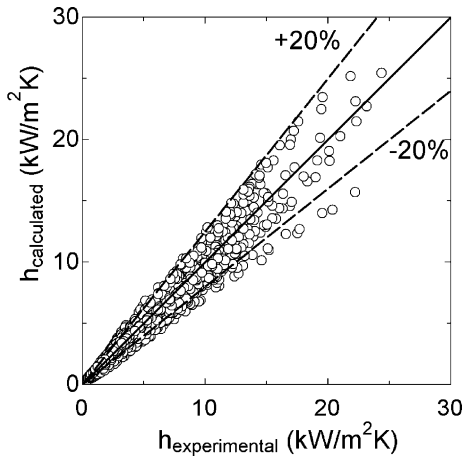


Fig. 9. Calculated versus experimental heat transfer coefficient for the complete set of data points.

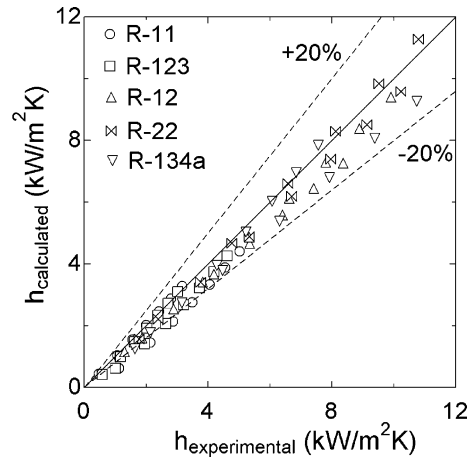


Fig. 11. Calculated versus experimental heat transfer coefficient for data from Webb and Pais [6].

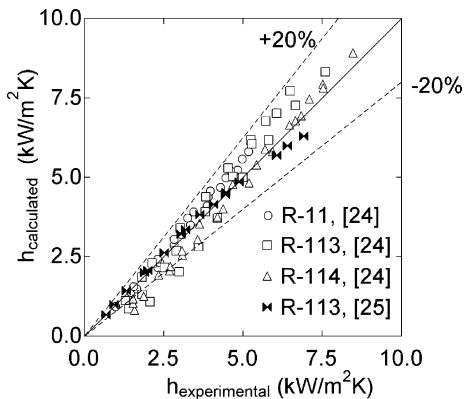


Fig. 10. Calculated versus experimental heat transfer coefficient for data from Silva [24] and Jensen [25].

Jensen [25]. It can be noted that most of the data points fall within the $\pm 20\%$ range. The correlation compares reasonably well with data from Silva [24] and Jensen [25] despite the surface roughness adjustments considering that: (1) the average surface roughness fitted for each set of data is in close agreement with the expected one for surfaces with similar finishing; (2) their data include refrigerants different from those used in the development of the present correlation; (3) the calculated heat transfer coefficient is in reasonable agreement with the experimental one.

Data from Webb and Pais [6] for the same refrigerants considered in this paper boiling on a commercial copper tube of 19 mm of external diameter have also been considered for comparison. Webb and Pais fitted their experimental data through equations having the following general form: $h = \text{Constant} \cdot \phi^m$ for each reduced pressure. The surface roughness was not pro-

vided. The average roughness, R_a , for a commercial copper tube was determined by averaging the average roughness of 10 different areas of 10 commercial copper tube samples, resulting a value equal to $0.6 \pm 0.2 \mu\text{m}$. Fig. 11 shows the comparison between the calculated versus the experimental heat transfer coefficient. It can be noted that the data points fall well within the $\pm 20\%$ range, a result that could be deemed quite reasonable, considering that neither the constant nor the roughness parameter of the proposed correlation have been adjusted to the experimental data.

8. Conclusions

A summary of the conclusions drawn from the results of the present experimental investigation involving the nucleate boiling of halocarbon refrigerants on cylindrical surfaces of different materials and conditions is as follows:

- (1) As a general rule, the nucleate boiling heat transfer coefficient of higher pressure refrigerants (R-12, R-22 and R-134a) is higher than that of lower pressure refrigerants (R-11 and R-123).
- (2) The reduced pressure and surface material and roughness affect the boiling curve in a degree that strongly depends on the particular refrigerant.
- (3) Nucleate boiling heat transfer is more intensely affected at reduced pressures and surface roughness.
- (4) The material of the heating surface affects the boiling curves in a combined fashion with the particular refrigerant. Transient conduction effects in the material seem to affect marginally the boiling curve.
- (5) Intermittence in the boiling pattern has been observed in the heat flux range between 10 and 20

kW/m². This phenomenon is characterized by alternate appearance and disappearance of bubble clusters in several regions of the boiling surface, and is particularly intensified in stainless steel.

- (6) The correlations proposed by Cooper [13], Stephan and Abdelsalam [14], and VDI-Heat Atlas [15] compare reasonably well with data from the present investigation, with absolute average deviations being in the 20% range.
- (7) Different forms of a generalized nucleate boiling heat transfer expression have been used in fitting the experimental data. The final form met several conditions proposed to objectively determine the best fitting correlation. It has been found that the overall average deviation of correlation with respect to the experimental heat transfer coefficient is equal to 9.6%. In addition, for evaluation purposes, the proposed correlation has been compared to results obtained elsewhere with resulting deviations being in the $\pm 20\%$ range.

Acknowledgements

The authors gratefully acknowledge the support given to the reported research by the Fundação de Amparo à Pesquisa do Estado de São Paulo, FAPESP, Brazil. The technical support given to this investigation by Mr. José Roberto Bogni is also appreciated and recognized.

References

- [1] M.G. Cooper, Correlations for nucleate boiling—formulation using reduced properties, *PCH Physicochem. Hydrodyn.* 3 (1982) 89–111.
- [2] D. Gorenflo, P. Hbner, W. Fust, A. Luke, E. Danger, U. Chandra, Pool boiling heat transfer and bubble formation of natural refrigerants on horizontal tube, in: *Proceedings of Joint Conference of the International Institute of Refrigeration Sections B and E*, University of Purdue, West Lafayette, Indiana, 2000.
- [3] M.G. Kang, Effects of surface roughness on pool boiling heat transfer, *Int. J. Heat Mass Transfer* 43 (2000) 4073–4085.
- [4] G. Ribatski, Theoretical and experimental analysis of pool boiling of halocarbon refrigerants, Doctoral thesis, Escola de Engenharia de São Carlos, University of São Paulo, Brazil 2002.
- [5] R.B. Abernethy, J.W. Thompson, *Handbook Uncertainty in Gas Turbine Measurements*, Arnold Engineering Development Center, Arnold Air Force Station, Tennessee, 1973.
- [6] R.L. Webb, C. Pais, Nucleate pool boiling data for five refrigerants on plain, integral-fin and enhanced tube geometries, *Int. J. Heat Mass Transfer* 35 (1992) 1893–1904.
- [7] H.M. Kurihara, Fundamental factors affecting boiling coefficients, PhD thesis, Purdue University, Lafayette, Indiana 1956.
- [8] Y.Y. Hsu, On the size range of active nucleation cavities on a heating surface, *J. Heat Transfer, ASME Series C* 84 (1962) 207–216.
- [9] C.Y. Han, P. Griffith, The mechanism of heat transfer in nucleate pool boiling—Part I, *Int. J. Heat Mass Transfer* 8 (1965) 887–904.
- [10] W.M. Rohsenow, A method of correlating heat transfer data for surface boiling liquids, *Trans. ASME* 74 (1952) 969–976.
- [11] M. Man, K. Stephan, P. Stephan, Influence of heat conduction in the wall on nucleate boiling heat transfer, *Int. J. Heat Mass Transfer* 43 (2000) 2193–2203.
- [12] D. Gorenflo, A. Luke, W. Künstler, M. Buschmeier, Prediction of pool boiling heat transfer with new refrigerants, in: *Proceedings of the CFC's the day after*, Padova, 1994, September 21–23, pp. 557–563.
- [13] M.G. Cooper, Heat flow rates in saturated nucleate pool boiling—A wide ranging examination using reduced properties, *Adv. Heat Transfer* 16 (1984) 157–238.
- [14] K. Stephan, M. Abdelsalam, Heat-transfer correlations for natural convective boiling, *Int. J. Heat Mass Transfer* 23 (1980) 73–87.
- [15] VDI-Heat Atlas, sixth ed., VDI-Verlag, Dusseldorf, 1994.
- [16] G. Ribatski, J.M. Saiz Jabardo, Nucleate boiling of halocarbon refrigerants—Heat transfer correlations, *Int. J. HVAC & R Res.* 6 (2000) 349–367.
- [17] H.K. Foster, N. Zuber, Bubble dynamics and boiling heat transfer, *AIChE J.* 1 (1955) 531–535.
- [18] N. Zuber, Nucleate boiling. The region of isolated bubbles and the similarity with natural convection, *Int. J. Heat Mass Transfer* 6 (1963) 53–78.
- [19] B.B. Mikic, W.M. Rohsenow, A new correlation of pool-boiling data including the effect of heating surface characteristics, *J. Heat Transfer* 91 (1969) 245–250.
- [20] K. Nishikawa, Y. Fujita, Correlation of nucleate boiling heat transfer based on bubble population density, *Int. J. Heat Mass Transfer* 20 (1977) 233–245.
- [21] S.I. Haider, R.L. Webb, A transient micro-convection model of nucleate pool boiling, *J. Heat Transfer* 40 (1997) 3675–3688.
- [22] W. Leiner, Heat transfer by nucleate pool boiling—general correlation based on thermodynamic similarity, *Int. J. Heat Mass Transfer* 37 (1994) 763–769.
- [23] B.E. Poling, J.M. Prauznitz, J.P. O'Connell, *The Properties of Gases and Liquids*, fifth ed., McGraw-Hill, New York, 2001.
- [24] C.L. Silva, Experimental investigation of the nucleate boiling of refrigerant–oil mixtures, Doctoral thesis, Escola Politécnica, University of São Paulo, Brazil 1989.
- [25] M.K. Jensen, Physical properties data tables and experimental boiling data, 1985, personal communication.